Available online at www.sciencedirect.com

SciVerse ScienceDirect

Energy Procedia 10 (2011) 292 – 296

Energy Procedia

European Materials Research Society Conference
Symp. Advanced Inorganic Materials and Concepts for Photovoltaics

Colloidal Crystals as Templates for Light Harvesting Structures in Solar Cells

E. Haugan[a,*], H. Granlund[b], J. Gjessing[a], E.S. Marstein[a]

[a]*Department of Solar Energy, Institute for Energy Technology, Instituttveien 18, 2007 Kjeller, Norway*
[b]*Department of Physics, Norwegian University of Science and Technology, Høgskoleringen 5, 7491 Trondheim, Norway*

Abstract

Monolayer colloidal crystals are formed using silica- and polystyrene beads and used as etch masks for the formation of regular, μm period hexagonal arrays of indentations in a silicon wafer. Such patterns can be used as diffraction gratings or as seeds for further processing, for example by pit-catalysed electrochemical etching. In another experiment, multilayer colloidal crystals are infiltrated with titania before subsequent removal of the beads, forming inverse opals displaying tuneable reflectivities which are interesting for use as selective reflectors.

Selection and/or peer-review under responsibility of Organizers of European Materials Research Society (EMRS) Conference: Symposium on Advanced Inorganic Materials and Concepts for Photovoltaics.

Keywords: light trapping, solar cells, nanosphere lithography, colloidal crystals, inverted opals, diffraction gratings

1. Introduction

The crystalline silicon solar cell industry is continuously moving towards thinner and thinner wafers as the production of solar cell grade silicon is a costly and energy intensive process. Thinner wafers are also beneficial because the collection efficiency of photogenerated free charges increases due to a shorter path way to the contacts. However, making a solar cell thinner allows more low-energy photons to pass through the entire structure without being absorbed, thus reducing efficiency. For this reason light harvesting (trapping) of low-energy photons is becoming an issue of increasing significance also for crystalline silicon solar cells. If the path length of photons inside the wafer can be increased by such light trapping structures, then the wafer can be made proportionally thinner without sacrificing efficiency. The most common light harvesting method in industry today is surface texturing by chemical etching, which scatters light into the solar cell due to refraction at the surface. This typically yields an average path length enhancement factor no greater than 10, which is only one fifth of the theoretical Lambertian limit for random scatterers in crystalline silicon [1].

*Corresponding author. Tel.: +47-95734413; fax: +47-63816356.
E-mail address: einar.haugan@ife.no

1876-6102 © 2011 Published by Elsevier Ltd. Selection and/or peer-review under responsibility of Organizers of European Materials Research Society (EMRS) Conference: Symposium on Advanced Inorganic Materials and Concepts for Photovoltaics. Open access under CC BY-NC-ND license.
doi:10.1016/j.egypro.2011.10.193

Periodic gratings with lattice periods close to photon wavelength may scatter light into non-zero diffraction orders, effectively increasing the path length of light inside the wafer. It has even been shown that the Lambertian limit can be exceeded by such geometries [2]. We have synthesised various periodic light harvesting structures for solar cell applications using colloidal crystal templates. 3D crystals are infiltrated with a dielectric material before the template is removed, leaving inverted opals displaying photonic band gaps giving sharp reflectivity peaks which make them interesting as selective reflectors. 2D crystals are used in nanosphere lithography for creating periodic patterns of pits, which may be used as diffraction gratings directly, or as initiation points or "seeds" for further processing into honeycomb-like structures by chemical or electrochemical etching.

2. Experimental

2.1. Substrate pre-treatment

Monocrystalline silicon wafers were used as substrates. Prior to template growth, the wafers were cleaned thoroughly using DI water and placed in a bath of DI water/NH_3(27%)/H_2O_2(30%), 515:85:100 volume ratio, at 70°C for 15 minutes. This was done to make the surface hydrophilic.

2.2. Colloidal crystal templates

In our experiments, 2D and 3D templates were grown from suspensions of microspheres purchased from Bangs Laboratories, Inc. Polystyrene (PS) beads gave the highest crystal quality and were therefore used when possible, while silica beads were used when high temperature processing was required. Bead diameters were selected for the optical properties of the final structures, determined by simulations [3, 4].

3D crystal synthesis. A 0.75 wt% solution of 490 nm diameter colloidal PS beads was prepared in a 25 ml glass beaker. The solution was thinned out to the desired concentration using DI water, before the glass beaker was placed in an ultrasonic bath for 15 minutes to break up any aggregates of colloidal spheres that may have formed.

Sphere self assembly was achieved using evaporation induced self assembly (EISA) [5]. Two cleaned substrates were inserted vertically into the beaker and placed in a heating cupboard for 24 hours at 63°C for the solvent to evaporate and the spheres to self-assemble on the substrate surface. According to Nagayama et al. [6] the growth rate v and hence the thickness of a multilayer colloidal crystal formed in this way depends on the volume fraction of solids in the solution, φ , as $v \propto \frac{\varphi}{1-\varphi}$. As the concentration of beads in the solution increases during deposition, it is therefore difficult to obtain homogeneous films by this method. Our samples typically showed a thickness variation from 10 layers (top) to 40 layers (bottom) of the substrate. For the optical properties, the thickness is not critical as long as it exceeds 5-8 layers [7]. Finally, the samples were sintered at the glass transition temperature of polystyrene (95°C) for 20 minutes.

2D crystal synthesis. Suspensions of 800 nm diameter silica beads were ultracentrifuged to increase the volume fraction of solids in water to approximately 30%. Solutions were sonicated for 5 hours at 24-27°C to break up aggregates, as suggested by Kumar [8] prior to spin-coating using a Bidtec SP100 spin coater. This was done by applying approximately 100 μl of solution onto a 1.5x1.5 cm^2 substrate, rotating the substrate to achieve full wetting, and then spin coating at 300 RPM for 1 second before increasing to 5500 RPM for 30 seconds. The same method was used for 1 μm PS beads, except only 5 minutes ultrasonication was needed.

2.3. 3D photonic crystals. Infiltration and inversion

With the 3D colloidal crystals in place, the next step is to fill the voids in the opal with a dielectric to enhance the refractive index contrast and thus maximize the band gaps. Infiltration with titania (TiO_2) was done using a Beneq TFS-500 atomic layer deposition machine. The precursors used were $TiCl_4$ (Aldrich 98%) and DI water. The chamber was purged using nitrogen of purity > 99.9999% between precursor pulses. The pulse/purge routine was: 0.25/0.75/0.25/0.75 seconds $TiCl_4$/purge/H_2O/purge. The deposition temperature was set to 85°C.

After infiltration, the PS colloidal sphere template was removed by calcination, leaving an inverse opal. This was done by heating to 525°C for 2 hours in a furnace with a 2 hour ramp-up. Besides removing the polystyrene, heat treating at these temperatures is reported to initiate the phase transition from amorphous titania to anatase [3].

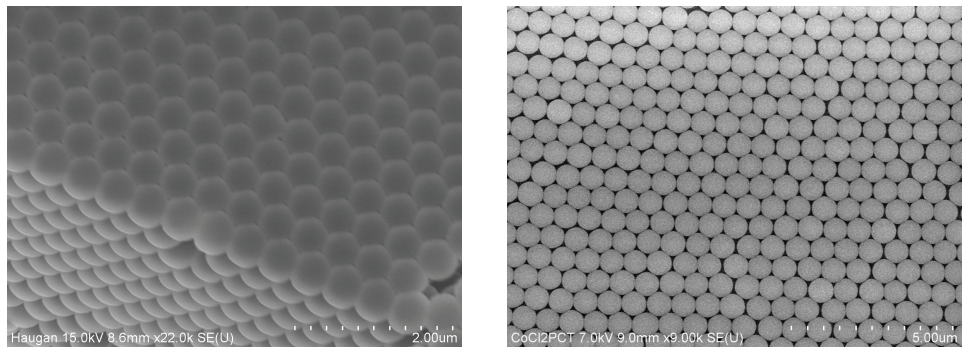

(a) Multilayer crystal (b) Single layer crystal

Figure 1: Scanning electron microscopy (SEM) images of the mono- and multilayer colloidal crystals synthesised

2.4. 2D photonic crystals by selective etching

In the first method, 50 nm of silicon nitride was deposited onto 2D colloidal crystals of silica beads to create an etch mask. The nitride was deposited using a Plasmalab System 133 PECVD at 400°C and 150 W RF power. After nitride deposition, the beads could be removed by sonication in ethanol for 2 minutes, leaving a silicon nitride etch mask. The substrates were then dipped in a 47% potassium hydroxide (KOH) solution for 30 seconds to etch pyramidic pits through the holes in the etch mask. At these conditions the etch rate along the {110} directions is approximately 700 nm/min [9, 10].

In the second method, monolayers of PS beads were covered by a 70 nm thick film of silver by thermal evaporation. The beads were removed by sonication, leaving behind triangular islands of silver. The samples were then submerged in a 4.6 M HF / 0.44 M H_2O_2 solution for 60 seconds. Silver is a catalyst for the etching of silicon by this solution.

3. Results

3.1. Colloidal crystal templates

3D crystal synthesis. The 3D crystals made were polycrystalline, with predominantly an hexagonal close packed ordering. This could be confirmed by laser diffraction experiments, looking at the reflection from the sample of a red laser beam of wavelength $\lambda = 650$ nm on a sand blasted plexiglass screen. The pattern of the reflected light showed clear hexagonal features, representing the Fourier transform of the structure. This would indicate that the real-space structure also has hexagonal symmetry [11]. Importantly, the laser spot size was so large that it would span across something in the order of 100 crystal domains, so the clear diffraction pattern indicates that adjacent domains maintained the same crystallographic orientation and packing conformation. Further corroboration of this comes from the fact that rotating the sample also caused the diffraction pattern to rotate accordingly. Thus, hexagonally close packed multilayer colloidal crystals could routinely be manufactured with thicknesses exceeding 10 layers.

2D crystal synthesis. The spin coating procedure produced a polycrystalline monolayer of spheres of predominantly hexagonal close-packed conformation, as seen in Figure 1 and confirmed by the presence of six-armed reflection patterns under white light. The monolayer quality was investigated in optical microscopy and scanning electron microscopy (SEM). Polycrystalline monolayers of PS beads covering typically 85% of the sample area were routinely manufactured, with the remaining area being mostly double layer. However for silica beads, agglomeration in solution prior to spin coating remained a problem even after several hours of ultrasonication at carefully controlled temperatures. Silica bead monolayers thus contained regions of poor quality in between crystal domains.

3.2. 3D photonic crystals. Infiltration and inversion

3D colloidal crystal templates were infiltrated with titania. Figure 2a shows the final structure after removal of the template. The refractive index of the relevant crystalline phases of titania have a refractive index in the range 2.3–3.0 in the wavelength range of interest. This contrast is too low to give rise to full photonic band gaps even after

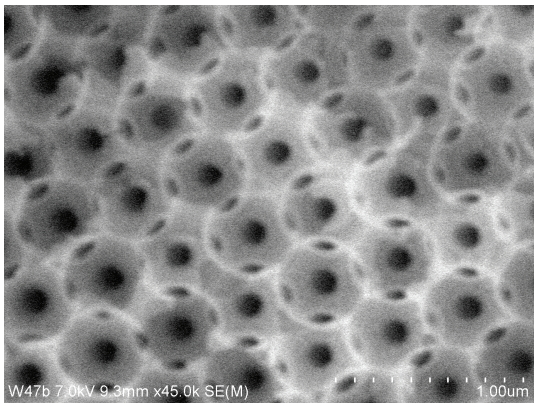

(a) SEM image of inverse titania opal

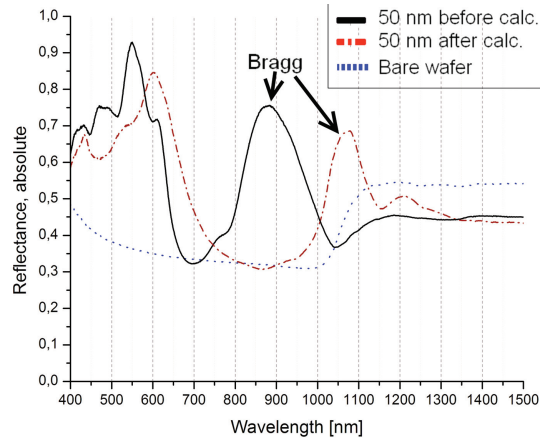

(b) Optical response of titania infiltrated opal before and after template removal by calcination. Interstices saturated with titania

Figure 2: Inverse titania opal. Template sphere diameter 490 nm

inversion of the opals. However, band structure simulations by King [12] predict several incomplete band gaps to arise following infiltration and inversion, detectable as peaks in the reflectivity spectrum.

Figure 2b shows the reflectivity of a titania infiltrated template. In addition to the Bragg peak, reflectivity peaks are also observed at high energies. After template removal (inversion) by calcination the refractive index contrast is increased, causing a blue shift of the reflectivity peaks. Also, some of the high-energy peaks get more pronounced. Templates with smaller diameter spheres gave similar reflectivity spectra, but with peaks at shorter wavelengths, demonstrating the size dependence of the band structure of these geometries.

We have achieved very good control and understanding of these structures, and we are able to tailor the reflectivity spectrum. However we also conclude that the band gaps, and thus the reflectivity peaks, are too narrow to be used as broad back reflectors in solar cells. We foresee that these structures are most relevant as spectral filters or selective reflectors in advanced solar cell applications.

3.3. 2D photonic crystals by selective etching

Method # 1. Silicon nitride etch masks, KOH etching. After nanosphere liftoff by sonication a thin layer of silicon nitride remained on the wafer, even in the "shadow regions" beneath the spheres. Atomic force microscopy (AFM) scans of these structures confirm the gradual thickness decrease of the nitride in the shadow region, forming a concave shape. Typical thickness variations from top to bottom of these concave shapes was 5 nm. At the bottom of each concave pit the bare silicon wafer was exposed in a 100 nm diameter patch, where the bead was touching the substrate.

Samples were then submerged in KOH, which etches crystalline silicon preferentially along the {110} directions. The etch does not attack silicon nitride, giving an essentially infinite etch selectivity [13]. Figure 3a shows a SEM image of a structure after KOH exposure and subsequent nitride stripping. This image reveals how the etching has indeed been confined to only the small exposed areas. Due to the high selectivity of the KOH etch on different crystallographic planes, etching is self-limiting.

Method # 2. Silver catalysed etching of silicon. AFM scans of the silver islands revealed that silver deposition was highly directional, as expected, with very little coverage in the shadow regions underneath the spheres. This is in sharp contrast to the nitride deposition in the previous section.

With the metal islands in place, samples were submerged in the HF / H_2O_2 etchant solution. As can be seen from Figures 3b and 3c, this method proved successful. From the top-down image, Figure 3b, we see that dark spots are formed where the silver islands used to be. The dark spots represent depressions in the wafer. The cross-sectional SEM image in Figure 3c demonstrates that the sidewall profile is indeed very straight, with no appreciable widening or narrowing of the groove. This is in line with the results by Huang et al [14]. Energy-dispersive X-ray spectroscopy (EDS) scans of the pits (Figure 3c, inset) show a high silver content at the bottom of the pits, as expected.

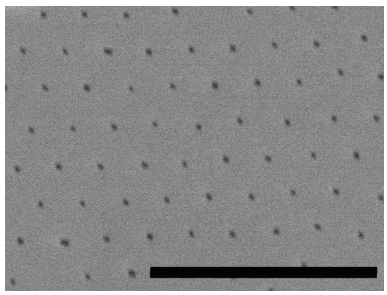

(a) Method # 1, after KOH etching and nitride stripping. Dark spots are pyramids etched out by the KOH. Scale bar 4 μm

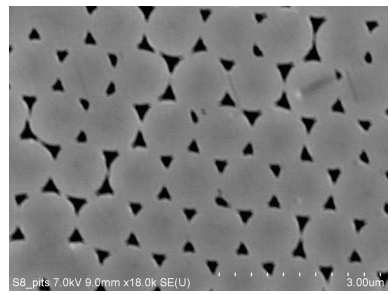

(b) Method # 2, metal catalysed pits (dark) seen from above

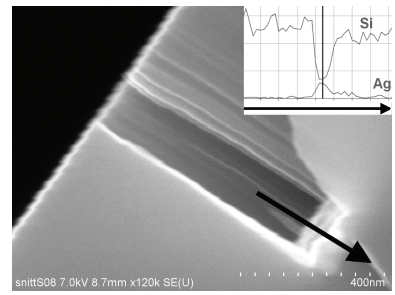

(c) Method # 2, metal catalysed pit seen from the side. The inset shows an EDS line scan (elemental analysis) along the arrow. At the bottom of the pit the silver concentration is high. 60 second etch

Figure 3: SEM images of etch pits, formed by the two methods

4. Conclusion

In conclusion, we have successfully manufactured single- and multilayer colloidal crystals on silicon wafers and used them as templates for the production of various geometries intended for light harvesting in solar cells. Specifically, we have made titania inverse opals displaying multiple reflectivity peaks whose wavelength position can be tuned by altering the degree of infiltration and template bead size. These structures are intended for use as selective reflectors in advanced multilayer solar cells. Also, we have demonstrated two different techniques for the formation of hexagonal arrays of dents or dimples in a wafer. These methods can either be used to form 2D light harvesting structures directly, or to form initiation points ("seeds") for further processing into honeycomb structures by chemical- or electrochemical etching. Specifically, silicon nitride etch masks were made by nanosphere lithography, displaying 100 nm diameter holes with a sub-micron pitch. These masks were then used as etch masks for KOH etching, forming pyramidal dents in the exposed wafer. Silver catalysed etching was also used to form hexagonal arrays of pits.

References

[1] J. Nelson, The Physics of Solar Cells, Imperial College Press, London, 2003.
[2] Z. Yu, A. Raman, S. Fan, Fundamental limit of light trapping in grating structures, Optics Express 18 (103) (2010) A366–A380.
[3] J. King, D. Heineman, E. Graugnard, C. Summers, Atomic layer deposition in porous structures: 3D photonic crystals, Applied Surface Science 244 (1-4) (2005) 511–516.
[4] J. Gjessing, A. Sudbø, E. Marstein, Comparison of periodic light-trapping structures in thin solar cells, Journal xx (2011) xx, submitted for publication.
[5] P. Jiang, J. Bertone, K. Hwang, V. Colvin, Single-crystal colloidal multilayers of controlled thickness, Chem. Mater 11 (8) (1999) 2132–2140.
[6] A. Dimitrov, K. Nagayama, Continuous convective assembling of fine particles into two-dimensional arrays on solid surfaces, Langmuir 12 (5) (1996) 1303–1311.
[7] H. Granlund, Fabrication of a photonic crystal using self-assembly. a potentially new rear reflector in solar cells, Master's thesis, NTNU, Trondheim, Norway (2009).
[8] K. Kumar, Preparation and characterization of spin-coated colloidal templates and patterned electrodeposited cobalt, Ph.D. thesis, Memorial University of Newfoundland (2008).
[9] H. Seidel, L. Csepregi, A. Heuberger, H. Baumgartel, Anisotropic etching of crystalline silicon in alkaline solutions, J. Electrochem. Soc 137 (11) (1990) 3612–3626.
[10] K. Mangersnes, Back-contacted back-junction silicon solar cells, Ph.D. thesis, University of Oslo (2010).
[11] A. Sinitskii, V. Abramova, T. Laptinskaya, Y. Tretyakov, Domain mapping of inverse photonic crystals by laser diffraction, Physics Letters A 366 (4-5) (2007) 516–522.
[12] J. King, Fabrication of opal-based photonic crystals using atomic layer deposition, Ph.D. thesis, Georgia Institute of Technology (2004).
[13] K. Williams, K. Gupta, M. Wasilik, Etch rates for micromachining processing-Part II, Microelectromechanical Systems, Journal of 12 (6) (2003) 761–778.
[14] Z. Huang, H. Fang, J. Zhu, Fabrication of silicon nanowire arrays with controlled diameter, length, and density, Advanced Materials 19 (5) (2007) 744–748.